Identification of Anxiolytic/Nonsedative Agents among Indol-3-ylglyoxylamides Acting as Functionally Selective Agonists at the γ-Aminobutyric Acid-A ($GABA_A$) α_2 Benzodiazepine Receptor

Sabrina Taliani,[†,*] Barbara Cosimelli,[‡,*] Federico Da Settimo,[†] Anna Maria Marini,[†] Concettina La Motta,[†] Francesca Simorini,[†] Silvia Salerno,[†] Ettore Novellino,[‡] Giovanni Greco,[‡] Sandro Cosconati,[‡] Luciana Marinelli,[‡] Francesca Salvetti,[§] Gianluca L'Abbate,[§] Silvia Trasciatti,[§] Marina Montali,[⊥] Barbara Costa,[∥] and Claudia Martini[⊥]

Dipartimento di Scienze Farmaceutiche, Università di Pisa, Via Bonanno 6, 56126 Pisa, Italy, Dipartimento di Chimica Farmaceutica e Tossicologica, Università di Napoli "Federico II", Via Domenico Montesano 49, 80131 Napoli, Italy, Abiogen Pharma SpA, Research Centre, Via del Paradiso 6, 56019 Migliarino Pisano, Pisa, Italy, Dipartimento di Psichiatria, Neurobiologia, Farmacologia e Biotecnologie, Università di Pisa, Via Bonanno 6, 56126 Pisa, Italy, Dipartimento di Morfologia Umana e Biologia Applicata, Università di Pisa, Via Volta, 4, 56126 Pisa, Italy

Received January 29, 2009

Anxioselective agents may be identified among compounds binding selectively to the $\alpha_2\beta_x\gamma_2$ subtype of the γ-aminobutyric acid-A ($GABA_A$)/central benzodiazepine receptor (BzR) complex and behaving as agonists or among compounds binding with comparable potency to various BzR subtypes but eliciting agonism only at the $\alpha_2\beta_x\gamma_2$ receptor. Because of subtle steric differences among BzR subtypes, the latter approach has proved much more successful. A biological screening within the class of indol-3-ylglyoxylamides **1**−**3** allowed us to identify compounds **1c** and **2b** as potential anxiolytic/nonsedative agents showing α_2 selective efficacy in vitro and anxioselective effects in vivo. According to molecular modeling studies, and consistently with SARs accumulated in the past decade, 5-NO_2− and 5-H-indole derivatives would preferentially bind to BzR by placing the indole ring in the L_{Di} and the L_2 receptor binding sites, respectively.

Introduction

Benzodiazepines are currently the drugs of first choice in the treatment of anxiety. These compounds bind to an allosteric site located at the γ-aminobutyric acid-A ($GABA_A$[a]) receptor complex, the so-called central benzodiazepine receptor (BzR).[1] Actually, benzodiazepines represent just one of the many chemically diverse classes of ligands of the $GABA_A$/BzR complex that display a pharmacological action ranging from full agonism (anxiolytic, anticonvulsant, sedative-hypnotic, and myorelaxant agents) to antagonism (agents to reverse sedation caused by BzR agonists), and to inverse agonism (anxiogenic, somnolytic, and proconvulsant agents). Agonists and inverse agonists are positive and negative allosteric modulators of GABA affinity, respectively, while antagonists do not modify GABA binding.[2,3]

The $GABA_A$/BzR complex contains a chloride channel and is a membrane-bound heteropentameric protein that may be assembled from at least 21 subunits belonging to eight different classes (6α, 4β, 4γ, 1ε, 1δ, 3ρ, 1θ, and 1π).[4−6] It has been found that a fully functional $GABA_A$/BzR must contain an α subunit, a β subunit, and a γ subunit, and it is currently accepted that the predominant native receptors comprise 2α, 2β, and 1γ subunits. The major benzodiazepine-sensitive $GABA_A$ receptor subtypes in the brain are $\alpha_1\beta_x\gamma_2$, $\alpha_2\beta_x\gamma_2$, $\alpha_3\beta_x\gamma_2$, and $\alpha_5\beta_x\gamma_2$, with the BzR being located between the α and γ subunits. The $\alpha_4\beta_x\gamma_2$ and $\alpha_6\beta_x\gamma_2$ subtypes do not respond to benzodiazepines and are therefore called benzodiazepine-insensitive receptors.[7] The γ_2 subunit is the major occurring γ subunit in the brain. The β subunit does not seem to affect the pharmacology of benzodiazepines, whereas it has been demonstrated that the α subunit is the main determinant of BzR ligand selectivity (therefore BzR subtypes take their names from the α subunit).[7−9] In situ mRNA hybridization, subunit specific immunoprecipitation, and immunoaffinity chromatography have allowed the determination of the distribution of the $GABA_A$ subtypes in the brain. The $\alpha_1\beta_x\gamma_2$ subtypes are the dominant ones and are present in both the cerebellum and the cortex. The $\alpha_2\beta_x\gamma_2$ and $\alpha_3\beta_x\gamma_2$ receptors are of medium abundance and are found mainly in the cortex and hippocampus, whereas the $\alpha_5\beta_x\gamma_2$ isoforms are scarcely abundant as they are only largely expressed in the hippocampus. This differential localization of the $GABA_A$ receptor subtypes in brain areas has suggested that the different subtypes may be associated with different physiological effects. In particular, it was demonstrated that the α_1 containing BzR mediates sedative action, that the α_2 subtype is involved in anxiolytic and myorelaxation effects, and that the α_5 subtype is associated with cognition processes like learning and memorizing. Finally, the role of the α_3 subtype seems to be mainly involved in mediating anxiety.[7−9] The correlation between pharmacological profile and specific action at the various BzR subtypes provides a rationale for the search of molecules capable of binding and/or eliciting allosteric modulation at a single or a group of BzR subtype/s. Thus, an anxioselective BzR ligand may be identified either among compounds binding selectively to the α_2 subtype and behaving as agonists (affinity-based selective agents) or among compounds binding with comparable

* To whom correspondence should be addressed. For S.T.: phone, +390502219547; fax, +390502219605; E-mail, taliani@farm.unipi.it. For B.C.: phone, +39081678614; fax, +39081678630; E-mail, barbara.cosimelli@unina.it.

† Dipartimento di Scienze Farmaceutiche, Università di Pisa.

‡ Dipartimento di Chimica Farmaceutica e Tossicologica, Università di Napoli "Federico II".

§ Abiogen Pharma SpA, Research Centre.

∥ Dipartimento di Morfologia Umana e Biologia Applicata, Università di Pisa.

⊥ Dipartimento di Psichiatria, Neurobiologia, Farmacologia e Biotecnologie, Università di Pisa.

[a] Abbreviations: GABA, γ-aminobutyric acid; BzR, central benzodiazepine receptor; LD test, light−dark test; MD, molecular dynamics.

10.1021/jm9001154 CCC: $40.75
Published on Web 05/26/2009

Chart 1. Structures of Indol-3-ylglyoxylamide Derivatives **1**−**3**

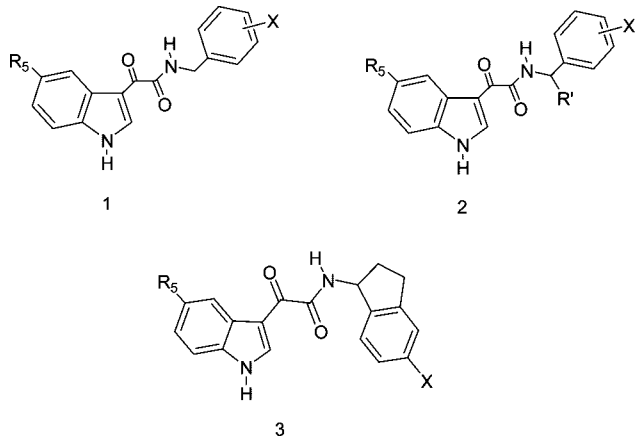

potency to various BzR subtypes that elicit agonism at the α_2 subtype and antagonism at other subtypes (efficacy-based selective agents). Compared to classical nonspecific BzR agonists, such as diazepam, either affinity or efficacy-based α_2 selective agonists are expected to retain anxiolytic properties without side effects like sedation, ataxia, tolerance, dependence, and impairment of cognitive processes.[10,11]

Molecular modeling studies performed by Cook's group[12] on structurally different classes of BzR ligands led to the development of a comprehensive pharmacophore/topological model consisting of several BzR interaction (sub)sites: (i) an H-bond acceptor (A_2), (ii) an H-bond donor (H_1), (iii) an H-bond donor/acceptor (H_2/A_3), (iv) four lipophilic pockets (L_1, L_2, L_3, and L_{Di}), and (v) three sterically forbidden sites (S_1, S_2, and S_3) as boundaries of the receptor binding cleft.

Further studies by the same researchers have suggested that the shapes of the BzR subtypes are very similar, with the exception of α_1 and α_5 subtypes that seem to be slightly larger in size at two distinct lipophilic regions, called L_{Di} and L_2 regions, respectively.[13] The above steric differences have been exploited to obtain ligands that bind selectively to either α_1 or α_5 subtypes[14] but have also hampered the identification of affinity-based α_2 and/or α_3 selective ligands.[15] The search of efficacy-based α_2 and/or α_3 selective ligands by screening and lead optimization methods has yielded better results in a variety of chemical classes.[10,16−25]

In the past several years, our research group has described the synthesis and biological evaluation of several BzR ligands featuring an indol-3-ylglyoxyl scaffold: *N*-benzylindol-3-ylglyoxylamides (**1**),[26] (*R*) and (*S*) enantiomers of *N*-(α-substituted-benzyl)indol-3-ylglyoxylamides (**2**),[27] and *N*-(indan-1-yl)indol-3-ylglyoxylamides (**3**)[27] (Chart 1). The structure−affinity relationships of these ligands were rationalized by assuming that they adopt two alternative binding modes, called A and B in their interaction with the BzR (Figure 1). Specifically, the 5-Cl/NO_2 derivatives adopt preferentially the binding mode A, whereas the 5-H derivatives preferentially adopt the binding mode B.[27,28]

Prompted by the interesting potency displayed by some of the indoles **1**−**3** at the wild type BzR, as well as their favorable pharmacokinetic properties,[28,29] we tested them as potential anxioselective agents in three steps: (i) determine the affinity for the rat recombinant $\alpha_1\beta_2\gamma_2$, $\alpha_2\beta_2\gamma_2$, and $\alpha_5\beta_3\gamma_2$ BzR subtypes, (ii) determine the efficacy profile for compounds displaying the highest potency at the α_2 BzR subtype, and (iii) evaluate the in vivo pharmacological properties of compounds that turned out to be affinity- or efficacy-based α_2 selective.

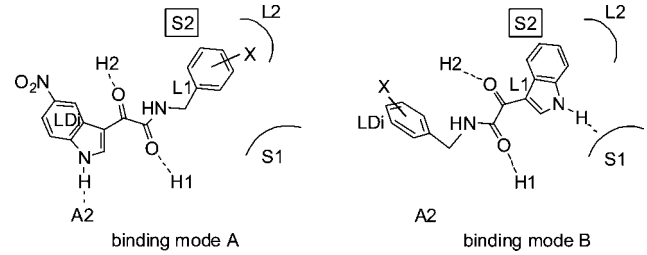

Figure 1. Hypothetical binding modes A and B of indole derivatives to BzR within the framework of Cook's pharmacophore/topological model.[27,28]

Scheme 1. Synthesis of Indol-3-ylglyoxylamide Derivatives **3c**−**j**

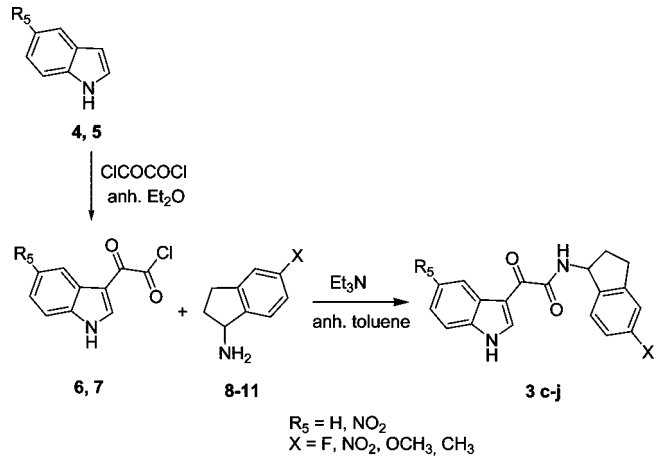

The same screening was then extended to newly synthesized derivatives of the relatively rigid *N*-(indan-1-yl)indol-3-ylglyoxylamide scaffold[27] bearing different substituents (X = F, NO_2, CH_3, OCH_3) at the 5′ position of the indane nucleus (compounds **3c**−**j**).

Herein, we describe the synthesis of the novel derivatives **3c**−**j** and the biological/pharmacological studies on a number of indoles **1**−**3** leading to the identification of functionally selective agonists of the α_2 BzR subtype characterized by in vivo anxioselective properties. Finally, molecular modeling studies were carried out to rationalize the structure−affinity relationships in the class of indol-3-ylglyoxylamides at the molecular level.

Chemistry. Acylation of the appropriate indoles **4** and **5** with oxalyl chloride,[30] followed by reaction of the indolylglyoxylyl chlorides **6** and **7** in toluene with the appropriate amines **8**−**11** under mild conditions and in the presence of triethylamine afforded the new compounds **3c**−**j** (Scheme 1).

The 1-indanamines **8**,[31] **10**,[32] and **11**[33] were prepared following a published synthetic procedure[33] starting from the corresponding 5-substituted-1-indanones, whereas the 5-nitro substituted derivative **9** was obtained in three steps according to another synthetic route (Scheme 2). The 5-nitro-1-indanone **13** was synthesized in good yield (66%) by oxidation of the 5-amino-1-indanone **12** with *m*-chloroperoxybenzoic acid in dichloromethane. Reaction of **13** with methoxyamine led to the intermediate methyloxime **14** that was converted into the final amine **9** by treatment with diborane in tetrahydrofuran. All 1-indanamines **8**−**11** were used as racemic mixtures.

Biological and Pharmacological Studies. The binding affinity of the newly synthesized indole derivatives **3c**−**j** for the BzR in bovine brain membranes was determined by

Scheme 2. Synthesis of 5-Nitro-1-indanamine **9**

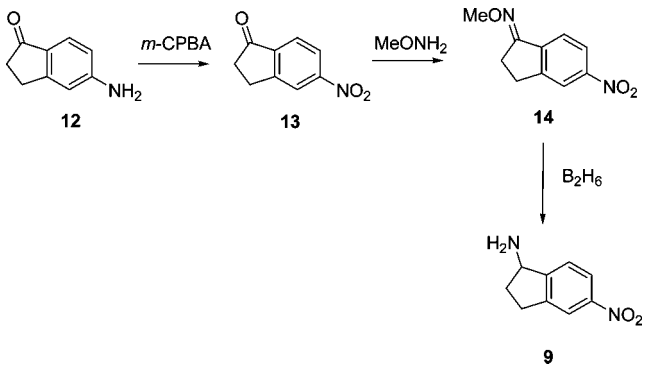

competition experiments against the radiolabeled antagonist [^{3}H]flumazenil[34] and expressed as K_i values only for compounds inhibiting radioligand binding by more than 80% at a fixed concentration of 10 μM (Table 1). The binding data of the previously described indol-3-ylglyoxylamides **1a**−**h**,[26] **2a**−**b**,[27] and **3a**−**b**[27] are also included in Table 1.

The affinity of compounds **3c**−**j** for BzR subtypes was evaluated by measuring their ability to displace [^{3}H]flumazenil in membranes from HEK293 cells expressing rat $\alpha_1\beta_2\gamma_2$, $\alpha_2\beta_2\gamma_2$, and $\alpha_5\beta_3\gamma_2$ BzRs (Table 1).[27] The same binding assays were performed for compounds **1c**−**h**,[26] **2a**−**b**,[27] and **3a**−**b**[27] **(**Table 1).

The compounds displaying the highest potency at the α_2 BzR (**1c**, **2b**, **3b**) were tested for their functional efficacy by measuring their modulatory effect on $^{36}Cl^-$ influx through the ion channel pore at a GABA concentration, evoking 20% of the maximum influx (EC_{20}) in cloned HEK293 cells expressing $\alpha_1\beta_2\gamma_2$ and $\alpha_2\beta_2\gamma_2$ BzRs, as previously described.[29,35] A 100 times higher concentration than the K_i value of the tested compound provided the maximal effect on the GABA-evoked Cl^- influx.[36] Efficacy results are shown in Figure 2, in which the nonselective full agonist diazepam was included as the reference standard.

Furthermore, the anxiolytic activity of the selected compounds **1c**, **2b**, and **3b** was first evaluated by a mouse light/dark (LD) test, after ip treatment with the test compound (20 mg/kg), or diazepam (1.25 mg/kg) used as control (Figure 3).

Molecular Modeling Studies. Docking simulations were carried out using the AutoDock4 (AD4) software.[37] Compounds **1c** and **2b** were docked into the models of the BzR constructed by Cromer et al.[38] and by Ernst et al.[39] The binary complexes between ligands and the receptor were further investigated by molecular dynamics (MD) simulations using the AMBER 9.0 package software.[40] Visual inspections of the calculated complexes were attained using the MGL Tools[41] and the UCSF Chimera packages.[42]

Results and Discussion

The binding data reported in Table 1 indicate that most of the newly synthesized compounds **3c**−**j** show appreciable affinity for the BzR in bovine brain membranes, with the 5-NO_2 substituted derivatives being more potent than the corresponding 5-H counterparts. Compound **3j**, bearing 5-NO_2 and 5′-OCH_3 substituents, stands out as the most potent in the whole series with a K_i value of 13 nM. The higher potency of **3j** (K_i 13 nM) compared with the parent compound **3b** (K_i 28 nM) may be due to an H-bond between the 5′-OMe group of **3j** (in the binding mode A) and an H-bond donor that we believe is present on the surface of the S_1 site.[43] Within the 5-H indanyl derivatives, the insertion of electron-withdrawing groups on the side chain of the aromatic ring does not improve the affinity, differently from the trend observed in the benzylamine series (compare **3c** and **3e** vs **3a**, with respect to **1c** and **1e** vs **1a**).

The novel compounds endowed with significant potency at the wild type BzR (**3c**,**d**,**f**,**i**,**j**), together with some previously described indoles (**1c**−**h**, **2a**,**b**, and **3a**,**b**), were assayed for their affinity to recombinant rat $\alpha_1\beta_2\gamma_2$, $\alpha_2\beta_2\gamma_2$, and $\alpha_5\beta_3\gamma_2$ BzRs (Table 1).

An overview of the binding data shows that all tested compounds display enhanced affinities for the α_1 isoform compared with α_2 and α_5 subtypes with various degrees of selectivity. The only exception is **1c**, which showed a moderate α_2 binding selectivity. However, a number of ligands (**1e**, **2b**, **3b**, **3j**) showed a fairly good α_2 binding affinity, even though they were not selective. These data indicate that the insertion of small groups with various steric and electronic properties on the side chain of the benzene ring (both in the benzylamines **1**,**2** and in their indanyl closed-chain analogues **3**) does not lead to a selective binding to the α_2 BzR.

As mentioned above, it has been widely reported in the literature how difficult it is to obtain affinity-based α_2 selective ligands due to subtle steric differences among BzR subtypes,[15] whereas efficacy-based α_2 selective agents have been more easily identified.[16,19,44] Thus, we assessed the efficacy profile of compounds **1c**, **2b**, and **3b**, displaying the highest potency at the α_2 BzR. Figure 2 shows the maximal efficacy on coapplication with GABA of the tested compounds at the rat recombinant α_1 and α_2 BzRs, using diazepam as the reference standard. At the α_1 subtype, all three compounds displayed an efficacy lower than the one of diazepam (11%, 35%, 1%, and 71% for **1c**, **2b**, **3b**, and diazepam, respectively). In particular, the efficacy ranged from antagonism for **3b** to partial agonism for **2b** and antagonism/partial agonism for **1c**. At the α_2 subtype, **1c** and **2b** showed an efficacy profile comparable to the one of diazepam (85%, 79%, and 81% for compounds **1c**, **2b**, and diazepam, respectively), whereas **3b** behaved as a partial agonist (48% and 81% for **3b** and diazepam, respectively). These results may predict anxiolytic nonsedative properties for the tested compounds.

Because of their promising efficacy profile, **1c**, **2b**, and **3b** were evaluated in vivo for their effects on mouse anxiety by means of a light/dark (LD) apparatus, using diazepam as the anxiolytic control.

The LD test is based on the mouse conflict between its innate aversion to brightly illuminated areas and its spontaneous exploratory behavior in response to mild stress, that is, novel environment and light. When given a choice between a large brightly lit compartment and a small dark compartment, a mouse spontaneously prefers the dark one. The conflict rises between the natural tendency to explore and the initial tendency to avoid the unfamiliar (neophobia). In this view, drug-induced increase in behaviors in the brightly lit open area is proposed to reflect anxiolytic activity.[45] The time spent in the lit area and the number of transitions between the light and dark chambers have been reported as the most reliable parameters to assess anxiolytic-like activity.[46−49] Another important parameter involves the evaluation of the total activity of the animals that could be considered as an index of potential sedative action. Thus, it seems obvious that animals that spend less time in one compartment demonstrate few movements and vice versa. To avoid this problem, results of movements/exploratory behavior in a specific area were expressed as a function of the time spent

Table 1. Inhibition of [^{3}H]Flumazenil Specific Binding to Bovine Brain Membranes and to Rat $\alpha_1\beta_2\gamma_2$, $\alpha_2\beta_2\gamma_2$, and $\alpha_5\beta_3\gamma_2$ $GABA_A$/Bz Receptor Subtypes[a] of Indol-3-ylglyoxylylamide Derivatives **1**−**3**

no.	R_5	R′	X	Conf.	K_i (nM)[b] or % inhibition (10 μM)[c]			
					cortex	$\alpha_1\beta_2\gamma_2$	$\alpha_2\beta_2\gamma_2$	$\alpha_5\beta_3\gamma_2$
					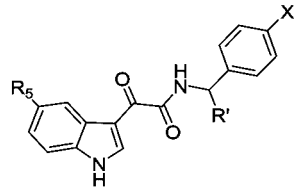			
1a	H	H	H	-	120 ± 11[d]	346 ± 29[e]	39% ± 3[e]	46% ± 5[e]
1b	NO_2	H	H	-	117 ± 12[d]	65 ± 5[e]	32% ± 3[e]	44% ± 4[e]
1c	H	H	F	-	52 ± 4[d]	245 ± 20	118 ± 10	163 ± 14
1d	NO_2	H	F	-	24% ± 3[d]	ND[f]	ND	ND
1e	H	H	NO_2	-	21 ± 2[g]	16 ± 2[g]	210 ± 15	58 ± 6[g]
1f	NO_2	H	NO_2	-	620 ± 49[g]	293 ± 17	2980 ± 272	2220 ± 180
1g	H	H	OCH_3	-	163 ± 12[d]	195 ± 16	1950 ± 156	30% ± 5
1h	NO_2	H	OCH_3	-	53 ± 5[d]	42 ± 3[g]	1645 ±114	126 ± 11[g]
2a	H	CH_3	H	*R*	1307 ± 124[g]	1150 ± 86[g]	1550 ± 132	5500 ± 360[g]
2b	NO_2	CH_3	H	*R*	17 ± 1[g]	14 ± 2[g]	121 ± 9	239 ± 21[g]
					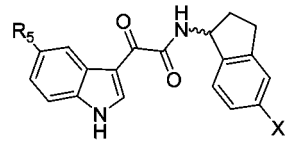			
3a	H	-	H	*R*	675 ± 31[g]	225 ± 13[g]	3100 ± 290	2160 ± 160[g]
3b	NO_2	-	H	*R*	28 ± 2[g]	9 ± 0.6[g]	85 ± 7	95 ± 8[g]
3c	H	-	F	*R/S*	2160 ± 168	2049 ± 180	29% ± 3	44% ± 3
3d	NO_2	-	F	*R/S*	300 ± 21	195 ± 10	810 ± 73	1420 ± 120
3e	H	-	NO_2	*R/S*	47%	ND	ND	ND
3f	NO_2	-	NO_2	*R/S*	178 ± 10	200 ± 15	513 ± 41	749 ± 65
3g	H	-	CH_3	*R/S*	15%	ND	ND	ND
3h	NO_2	-	CH_3	*R/S*	2%	ND	ND	ND
3i	H	-	OCH_3	*R/S*	636 ± 41	246 ± 19	690 ± 62	28% ± 2
3j	NO_2	-	OCH_3	*R/S*	13 ± 0.2	28 ± 0.5	231 ± 10	252 ± 14
diazepam					10 ± 1.1	11 ± 2.1	15 ± 1.7	9.8 ± 1.1
zolpidem					51 ± 4	50 ± 3	765 ± 63	35 ± 3

[a] The ability of the compounds to displace [^{3}H]flumazenil was measured in membranes from HEK293 cells expressing the $\alpha_1\beta_2\gamma_2$, $\alpha_2\beta_2\gamma_2$, and $\alpha_5\beta_3\gamma_2$ subtypes, as described in the Experimental Section. [b] K_i values are means ± SEM of three determinations carried out in triplicate. [c] Percentage inhibition values of specific [^{3}H]flumazenil binding at 10 μM concentration are means ± SEM of three determinations carried out in triplicate. [d] Data taken from ref 26. [e] Data taken from ref 29. [f] Not determined. [g] Data taken from ref 27.

in the compartment under consideration.[45] Anxiolytic agents selectively increased exploration rather than general activity.

In the present investigation, the time spent in the white compartment (TW), the number of transfers from the lit to the dark area and vice versa (Tran) were measured after the mouse was treated ip with the test compounds **1c**, **2b**, and **3b** (20 mg/kg) or diazepam (1.25 mg/kg) used as control (Figure 3a,b).

To evaluate the total activity parameter, the number of exploratory rearings in the white section and the number of line crossings (total activity, AW, data not shown) were also measured and expressed as a function of TW (AW/TW, Figure 3c).

Administration of the reference diazepam at a dose of 1.25 mg/kg produces anxiolytic-like effects, as evidenced by the significant increase of TW and Tran parameters with respect to vehicle treated group (Figure 3a,b). These results are in agreement with the literature.[46] This anxiolytic effect is devoid

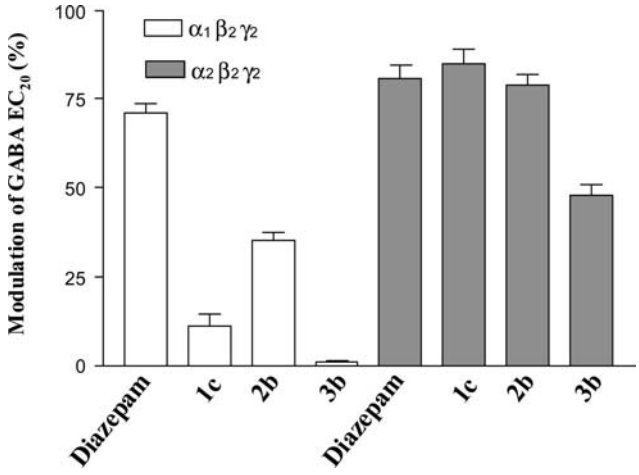

Figure 2. Maximal efficacy of compounds **1c**, **2b**, and **3b**, and diazepam on rat recombinant $\alpha_1\beta_2\gamma_2$ and $\alpha_2\beta_2\gamma_2$ $GABA_A$ receptor subtypes. Results are expressed as percentage of increase in the response to $GABA_A$ at EC_{20} (mean ± SEM) from at least five independent experiments.

of sedative component, as demonstrated by the AW/TW parameter that is even greater than the ones of the control group (Figure 3c).

Administration of compounds **1c** and **2b** in mice induced an increase in the TW and Tran values compared to vehicle-treated mice (Figure 3a,b); however, the AW/TW parameter for both compounds and control are comparable (Figure 3c). On the basis of these in vivo data, **1c** and **2b** may be novel anxiolytic agents lacking sedative activity.

In spite of its in vitro efficacy at the α_2 BzR, **3b** displayed no significant differences in vehicle-treated animals for all parameters measured, evidencing no appreciable in vivo activity (Figure 3). In this respect, the in vivo effects of pharmacologically active substances may diverge from those expected on the basis of in vitro experiments due to unfavorable pharmacokinetic properties (for example, **3b** may be metabolized to a different extent than **1c** and **2b**).

Molecular Modeling. Recently, Cook et al.[50] have oriented the previously proposed pharmacophore model[12,51] into the binding site of the $\alpha_1\beta_2\gamma_2$ BzR by considering the most recent advances in ligand structure−affinity relationships and structural studies of the receptor binding site. Taking into account this unified pharmacophore/receptor model, we undertook a molecular modeling study on our compounds in order to explain their structure−affinity relationships.

Among the available models of $\alpha_1\beta_2\gamma_2$ BzR in its closed-channel conformation (Figure 4), we considered those kindly provided by Cromer[38] and Ernst.[39] A detailed comparison of the two reveals that they share a common general folding, although, as expected, some differences can be seen in the orientation of the loops. Both these BzR models, most precisely the ligand binding domains of the α and γ subunits, were used to dock compounds **1c** and **2b** that were the most interesting from a pharmacological point of view. Results of docking simulations were analyzed by taking into account the predicted binding free energy (ΔG_{AD4}) associated to each docked solution, together with the consistency with ligand structure−affinity relationships data and results of receptor site-directed mutagenesis studies.

In particular, because experimental data have outlined that both the α and γ subunits are required for recognition and binding of BzR ligands,[52,53] all the docked poses in which the ligand was unable to efficiently contact both subunits at the same time were discarded.

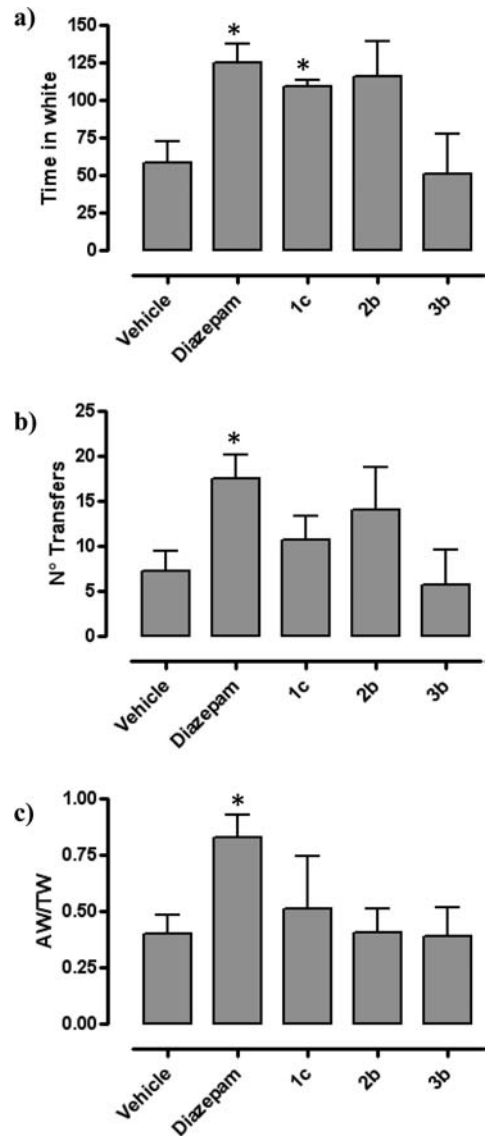

Figure 3. Effects of compounds **1c**, **2b**, and **3b** (20 mg/kg ip) on behavioral parameters in the LD test in mice ($n = 4-6$) in comparison with diazepam (1.25 mg/kg ip) or with vehicle (1% carboxymethyl cellulose). Each value represents mean ± SEM. Statistical significance was calculated for each substance versus the control using a two-tailed unpaired *t*-test. Mice that failed to move from the white to the black compartment were eliminated from the final analysis. * $p < 0.05$.

All the remaining solutions found for **2b** using Cromer's model belong to the two lowest energy clusters (the predicted binding free energies are reported in Table 4 in Supporting Information) and differ for the relative positions of the ligand aromatic rings. In the first cluster (mode A) **2b** projects its indole ring toward the γ subunit in the putative L_{Di} site ($Y160_\alpha$, $T142_\gamma$, $L140_\gamma$, $M130_\gamma$, and $R132_\gamma$)[50] and the phenyl ring is closer to the α subunit lying in the putative L_2 site (interface between loop C and A of the α subunit).[50] In the second cluster (mode B), the ligand aromatic rings are swapped (for any details of ligand−receptor interactions see Figure 1 in the Supporting Information). Interestingly, the existence of two possible binding modes for the indole derivatives had already been postulated in our previous studies based exclusively on their structure−affinity relationships.[28]

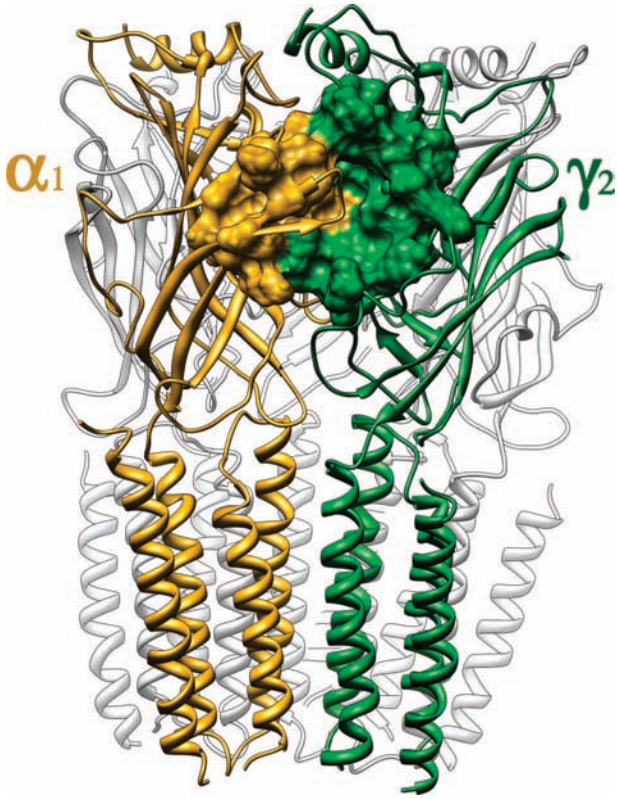

Figure 4. Side view of the used BzR model. The putative ligand binding cavity is depicted as a surface while the rest of the protein as ribbons. The α and γ subunits are colored as orange and green, respectively.

However, when the docking of **2b** was performed in the structural model of a α_1 BzR by Ernst and co-workers,[39] the ligand was unable to take direct contact with both the α and γ subunits at the same time. Particularly, in the great majority of the calculated binding poses, the ligand is closer to the α subunit. Such a behavior is mainly ascribable to the presence of $Q204_\alpha$ that extends its bulky side chain toward the inner part of the binding site preventing the ligand to span from the L_2 to the L_{Di} site. Similar considerations could also be done when Ernst's model was used to dock compound **1c**. Thus, Cromer's model was selected for further ligand−receptor model refinements.

Similarly to **2b**, when **1c** was docked in Cromer's model, a double binding pose was still found with the indole ring pointing toward the γ subunit (in the L_{Di} site, mode A) or toward the α one (in the L_2 pocket, mode B) (Figure 2 in Supporting Information).

The binary complexes calculated by the docking program for **1c** and **2b**, in both modes A and B, were then subjected to a 10 ns MD simulations to refine the predicted binding geometries. Most importantly, given the dichotomy of binding modes (A and B) predicted for these ligands, results of MD simulations could suggest a preferential binding orientation for each ligand.

Because in the present study only the extracellular portion of the BzR ligand binding domain was considered, a preliminary analysis of MD results was attained to probe whether the absence of the other BzR subunits (two β and one α) might have influenced the overall binding site architecture. To identify the relative internal motions of the protein residues, the isotropic temperature (B) factor for each residue in the simulations was calculated (see Figures 8 and 9 in Supporting Information). As expected, the truncation of the model led to a high degree of flexibility of the regions in direct contact with the missing segments. However, such an artifactual plasticity did not affect the conformation of the ligand binding site, as demonstrated by the low B-factor values calculated for the residues in this portion (see Figures 8 and 9 in Supporting Information). Thus, we are confident that considering the sole extracellular ligand binding domain does not significantly hamper the correctness of molecular modeling studies aimed at the description of a ligand binding mode in BzR.

For the **2b**/BzR complex in the binding mode A, the simulation demonstrated that the ligand is stabilized in a conformation similar to the starting one (Figure 5a and Supporting Information). In the L_{Di} site, the ligand 5-NO_2 group forms an H-bond with the $Y210_\alpha$ side chain (Figure 6a) that was found to be in direct interaction with other BzR ligands according to covalent labeling data.[54] Furthermore, during the MD simulations, an additional T-shaped interaction is established by the indole ring with $Y160_\alpha$ that is reinforced by the electron-withdrawing NO_2 group and by the formation of an H-bond between the ligand indole NH and the Y160α side chain OH.

Our **2b**/BzR interaction model is consistent with the pharmacophoric role of the indole NH as H-bond donor because its methylation as well as its replacement by an oxygen or a sulfur atom diminishes or abolishes the potency.[28,55] Moreover, the inspection of the energy-minimized average structure of the complex reveals the presence of an H-bond between the carbonyl oxygen attached to the indole ring and $S206_\alpha$. In such a conformation, the ligand side chain methyl group takes favorable hydrophobic contacts with $V203_\alpha$, $V213_\alpha$, and $H102_\alpha$. Additionally, the aromatic ring of $H102_\alpha$ is involved in a well-oriented T-shaped interaction with the ligand phenyl ring. According to structure−affinity relationships in the benzyl-3-indolylglyoxylamides, affinity is enhanced when the pendant phenyl ring is substituted at the 3′ and 4′ positions with hydroxy/methoxy groups (for instance, compare **3j** with **3b**). In this respect, a visual inspection of pose A calculated for **2b** reveals that $S205_\alpha$ (loop C) could indeed donate an H-bond to the above cited groups when they are present. The same is true for $K256_\alpha$. Moreover, it has been demonstrated that only the (*R*)-enantiomer of **2b** is endowed with affinity for BzR.[27] Indeed, the (*S*)-enantiomer of this ligand would hardly adopt pose A due to steric clashes between its phenyl ring and the α receptor subunit.

MD simulations for mode B have shown certain instability in the binding conformation calculated by AD4. In fact, during the production run, **2b** is displaced from its initial position and after 8 ns it adopts a stable orientation that differs substantially from the initial one (Figures 5b and 6b). Interestingly, the frames calculated in the last 3 ns of the simulations have the lowest potential energy values recorded during the production run. However, in this new binding pose, some inconsistencies arise from the position of the ligand phenyl ring that is now distant from the L_{Di} and that makes weak van der Waals contacts with $M81_\gamma$ and $L140_\gamma$ side chains in a rather shallow solvent exposed receptor region. Indeed, structure−affinity relationships data indicate that affinity is retained by replacing the phenyl ring with alkyl chains of suitable size and length, such as *i*-propyl or *n*-butyl but not longer or branched such as *n*-pentyl or *t*-butyl.[29] Likewise, replacement of the same phenyl moiety with different 5- or 6-membered aromatic rings allows retention of the affinity.[43] These data would suggest that the cleft hosting the benzyl moiety should be mainly hydrophobic and have a limited room. As mentioned before, while in mode A, the terminal phenyl of **2b** is placed in the lipophilic L_2 site, in mode B, the same ring is hosted in a rather shallow and large pocket

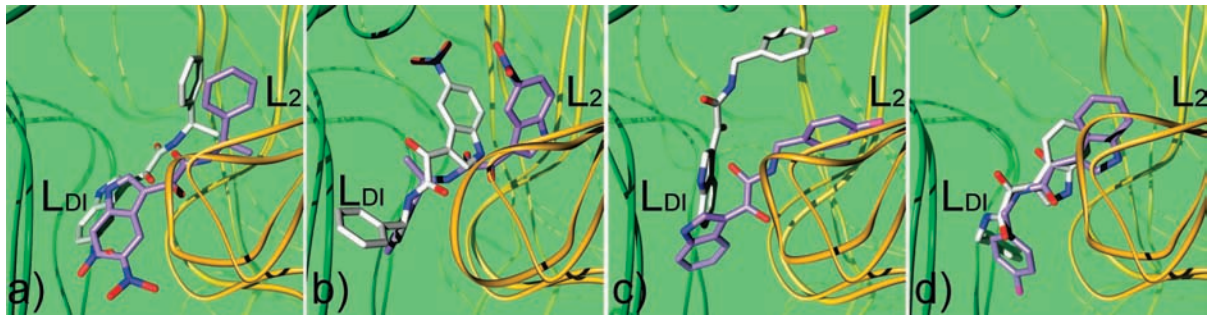

Figure 5. Binding conformations of **2b** (a and b) and **1c** (c and d) in pose A (a and c) and B (b and d) into the BzR cleft. The receptor is represented as green (γ subunit) and orange (α subunit) ribbons. Ligands in their docked conformations are represented in purple sticks, while ligands in conformations calculated through MD simulations are represented as white sticks.

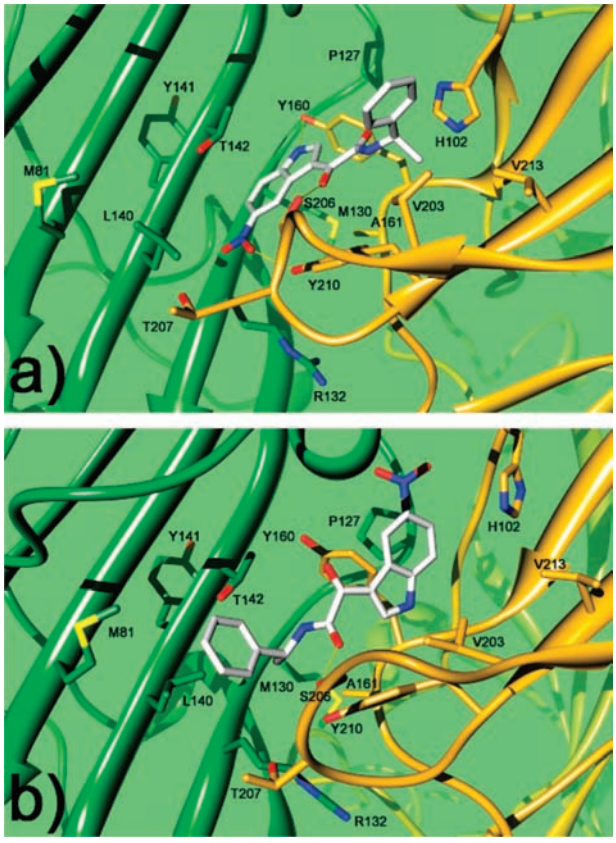

Figure 6. Energy-minimized average structures of the **2b**/BzR complex in binding modes A (a) and B (b). The ligand is depicted as white sticks, the α subunit as orange sticks and ribbons, and the γ one is represented as green sticks and ribbons. For clarity, only interacting residues are shown.

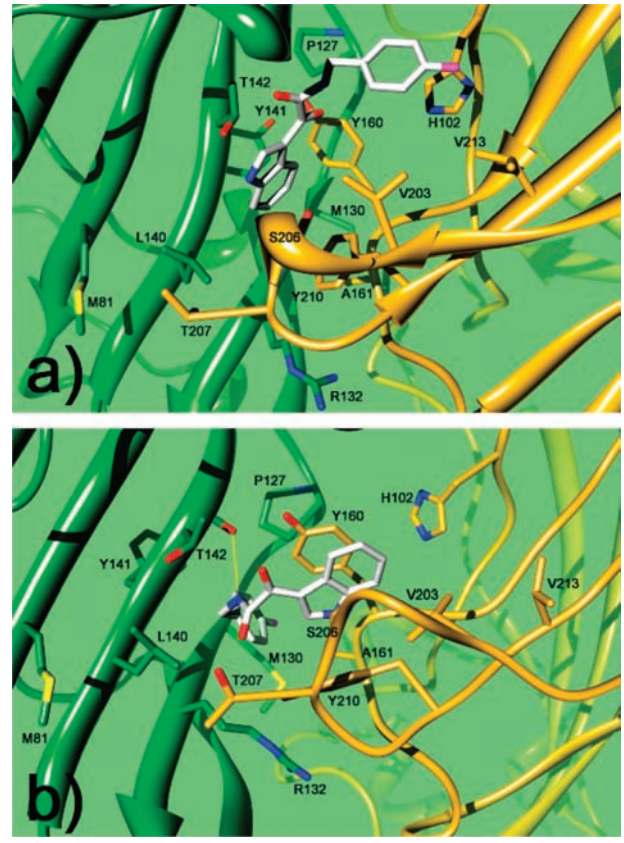

Figure 7. Energy-minimized average structures of the **1c**/BzR complex in binding modes A (a) and B (b). The ligand is depicted as white sticks, the α subunit as orange sticks and ribbons, and the γ one is represented as green sticks and ribbons. For clarity, only interacting residues are shown.

that can possibly host bulky substituents. From these considerations, mode A for **2b**, rather than B, seems to be more consistent with the above outlined experimental data.

Analysis of the MD trajectories for the **1c**/BzR complex in the binding mode A revealed that the ligand fluctuates among different orientations reaching after 6 ns a stable pose that is significantly different from the initial one (Figures 5c and 7a). Particularly, the ligand phenyl ring is displaced from the L_2 site in the α subunit to make weak contacts with loop F of the γ subunit (Figure 7a and Supporting Information).

During the 10 ns MD simulation of **1c** in the binding mode B, the ligand remains stably adapted in the receptor cavity (rmsd = 1.5 Å), contacting both α and γ subunits and having strong interactions (Figure 5d and Supporting Information). Specifically, the indole moiety is engaged in a $\pi-\pi$ interaction with the $Y160_\alpha$ aromatic ring, the *p*-fluorophenyl ring favorably contacts $M132_\gamma$, $Y141_\gamma$, $P127_\alpha$, and $A161_\alpha$ residues and engages a T-shaped interaction with the $Y160_\alpha$ side chain, and the amide NH donates an H-bond to the $T142_\gamma$ backbone CO (Figure 7b). Interestingly, for compounds of the 5-H indoles series, the replacement of the terminal benzyl moiety with various alkyl chains always results in a loss of potency.[29] This suggests the involvement of the pendant phenyl ring of these ligands in strong interactions with the receptor. Thus, pose B rather than A would be more consistent with structure−activity relationships in the 5-H indole series.

Interestingly, rescoring the minimized average complexes found in the MD simulations for **2b**/BzR and **1c**/BzR in the two binding solutions (A and B, respectively) with a new empirical scoring function implemented in AD_4,[37] we have

found that for **2b** pose A is energetically favored ($\Delta G = -7.0$ kcal/mol) over pose B ($\Delta G = -4.6$ kcal/mol) (Table 5 in Supporting Information). On the other hand, for compound **1c**, the AD4 rescoring predicted a ΔG value more favorable for pose B than for pose A (−8.5 and −5.1 kcal/mol, respectively). Analysis of the energy components of the four ΔG values reveals that the differences are mainly related to van der Waals contacts (corresponding to hydrophobic interactions) that are maximized in pose A for **2b** and in pose B for **1c** (Table 4 in Supporting Information).

Altogether, these results suggest that compound **2b** binds to the α/γ interface of the BzR adopting pose A, while **1c** preferentially adopts pose B in agreement with our previously reported pharmacophore/topological model.[27]

As reported in the present paper, **2b** and **1c** display a different efficacy profile at the BzR, with the first being a partial agonist and the second acting mostly as an antagonist. Nevertheless, we have not attempted to relate the different efficacies of these two compounds with their different putative binding modes to the BzR. So far, the molecular underpinnings responsible for the efficacy behaviors of indol-3-ylglyoxylamides, as well as of other classes of ligands of the BzR subtypes, still remain to be determined.

Conclusions

Anxioselective agents may be identified either among compounds binding selectively to the α_2 BzR subtype that behave as agonists or among compounds binding with comparable potency to various BzR subtypes that elicit agonism at the α_2 subtype and antagonism at other subtypes. Prompted by the success of the second approach, a number of indol-3-ylglyoxylamides belonging to our in-house collection were screened for their binding affinity to the rat recombinant α_1, α_2, and α_5 BzRs. Among the compounds with highest potency at the α_2 subtype, compounds **1c** and **2b** exhibited interesting properties either in vitro (full α_2 agonism and α_1 partial agonism/antagonism) or in vivo (anxiolytic/nonsedative activity in mice). Molecular docking calculations using a model of the BzR ligand binding domain in the closed state indicated the presence of two possible binding positions for **2b** and **1c** in which the ligand aromatic rings (indole and phenyl) can be alternatively lodged in the receptor L_2 and L_{DI} sites. Analysis of the stability of the predicted complex through MD simulations suggested that the presence of the 5-nitro group in **2b** would allow the formation of more productive interactions when the indole ring is embedded in the L_{Di} receptor region. Conversely, compounds devoid of such a substituent, as in **1c**, should produce more effective interactions when the indole ring is placed in the L_2 site.

Experimental Section

Chemistry. Melting points were determined using a Büchi apparatus B 540 and are uncorrected. Routine nuclear magnetic resonance spectra were recorded on a Varian Mercury 400 spectrometer operating at 400 MHz. EI-HRMS mass spectra were obtained on a Finnigan MAT95XP spectrometer using a direct injection probe and an electron beam energy of 70 eV. Evaporation was performed in vacuo (rotary evaporator). Analytical TLC was carried out on Merck 0.2 mm precoated silica gel aluminum sheets (60 F-254). Silica gel 60 (230−400 mesh) was used for column flash chromatography. Combustion analyses on target compounds were performed by our Analytical Laboratory in Pisa. All compounds showed ≥95% purity.

Besides the commercially available starting materials, the 5-substituted indanyl-1-amines **8**, **10**, and **11** were prepared in accordance with a reported method.[33]

General Procedure for the Synthesis of *N*-(Indan-1-yl)-(5-substituted indol-3-yl)glyoxylamide Derivatives 3c−j. Triethylamine (3.0 mmol) was added dropwise to a stirred suspension, cooled at 0 °C, of indolglyoxylyl chlorides **6** and **7** (2.5 mmol) and the appropriate amine **8**−**11** (2.75 mmol) in 50 mL of dry toluene. The reaction mixture was left to warm to room temperature, stirred for 24−48 h (TLC analysis), and then filtered. The precipitated collected was triturated with a saturated $NaHCO_3$ aqueous solution, washed with water, and collected again to give a first portion of crude product. The toluene solution was evaporated to dryness, and the residue was treated with saturated $NaHCO_3$ aqueous solution, washed with water, and collected to yield an additional amount of crude product. The quantities of amide derivatives obtained from the initial insoluble precipitate or from the toluene solution were variable depending upon the solubility of the various compounds. All products **3c−j** were purified by chromatography (chloroform:methanol = 9:1 v/v as eluant) and recrystallization from the appropriate solvent whenever a solid was obtained. Yields, recrystallization solvents, melting points, and spectral data are reported in the Supporting Information.

5-Nitro-1-indanone 13. A solution of 5-amino-1-indanone **12** (1.5 g, 10.2 mmol) in 10 mL of dichloromethane was treated at 0 °C with 1.75 g (10.2 mmol) of 51% *m*-CPBA (*meta*-chloroperoxybenzoic acid), and the mixture was stirred at the same temperature for 48 h. The organic solution was washed with a saturated $NaHCO_3$ aqueous solution, dried over Na_2SO_4, and evaporated to dryness. The obtained residue was purified by chromatography (dichloromethane as eluant) to obtain **13** as a yellow solid: yield 66%; mp 132−133 °C (lit.[56] 131−132.5 °C dec.). ^{1}H NMR (400 MHz, $CDCl_3$) δ 2.65−2.80 (m, 2H, 3-CH_2), 3.12−3.22 (m, 2H, 2-CH_2), 7.27−7.33 (m, 1H, H-7), 7.42−7.48 (m, 1H, H-4), 7.61−7.75 (m, 1H, H-6). Anal. ($C_9H_7NO_3$) C, H, N.

5-Nitroindan-1-methoxyimine 14. 5-Nitro-1-indanone **13** (1.3 g, 7.3 mmol) and methoxyamine hydrochloride (1.5 g, 18.2 mmol) were dissolved in a mixture of ethanol (15 mL) and pyridine (15 mL) and heated on a steam bath for 30 min. The solution was allowed to return to room temperature and then was diluted with water (30 mL) to precipitate practically pure **14**, which was collected by filtration: yield 84%; mp 174−176 °C. ^{1}H NMR (400 MHz, $CDCl_3$) δ 2.88−3.21 (m, 4H, 3-CH_2 and 2-CH_2), 4.02 (s, 3H, OCH_3), 7.55−7.70 (m, 1H, H-7), 8.13−8.33 (m, 2H, H-4 and H-6). Anal. ($C_{10}H_{10}N_2O_3$) C, H, N.

5-Nitro-1-indanamine 9. A solution of 5-nitroindan-1-methoxyimine **14** (1.3 g, 6.1 mmol) in 8 mL of THF was treated with 1 M diborane in THF (38.5 mL) and refluxed for 4 h in an argon atmosphere. Methanol (10 mL) was added and the solvent evaporated. The residue was treated with 10% HCl and heated on a steam bath for 30 min. The mixture was made alkaline with saturated $NaHCO_3$ aqueous solution and extracted with ethyl ether; the organic phase was dried (Na_2SO_4) and evaporated. The obtained residue was purified by chromatography (chloroform:methanol = 8:2 v/v as eluant), yielding the product **9** as a yellow solid: yield 35%; mp 279−281 °C. ^{1}H NMR (400 MHz, $CDCl_3$) δ 1.73−1.92 (m, 1H, H-2), 2.52−2.74 (m, 1H, H-2), 2.78−3.18 (m, 2H, 3-CH_2), 4.33−4.48 (m, 1H, H-1), 7.43−7.51 (m, 1H, H-7), 8.04−8.18 (m, 2H, H-4 and H-6). Anal. ($C_9H_{10}N_2O_2$) C, H, N.

Biological Methods. Materials. [^{3}H]Flumazenil (specific activity 70.8 Ci/mmol) was obtained from NEN Life Sciences Products. All other chemicals were of reagent grade and were obtained from commercial suppliers. HEK293 cells stably expressing rat $GABA_A$ receptor subtypes ($\alpha_1\beta_2\gamma_2$, $\alpha_2\beta_2\gamma_2$, $\alpha_5\beta_3\gamma_2$) were kindly supplied by Dr. François Besnard, Department of Molecular and Functional Genomics, Synthélabo, France.[57]

Radioligand Binding Studies. Bovine cerebral cortex membranes were prepared in accordance with ref 58. The membrane preparations were subjected to a freeze−thaw cycle, washed by suspension and centrifugation in 50 mM tris-citrate buffer pH 7.4 (T1), and then used in the binding assay. Protein concentration was assayed by the method of Lowry et al.[59] [^{3}H]Flumazenil binding studies were performed as previously reported.[27]

HEK293 cells stably expressing rat $GABA_A$ receptor subtypes ($\alpha_1\beta_2\gamma_2$, $\alpha_2\beta_2\gamma_2$, $\alpha_5\beta_3\gamma_2$) were maintained, as previously described,[57] in DMEM/Nut Mix F-12 with Glut-I (GIBCO), supplemented with 10% fetal bovine serum, L-glutamine (2 mM), penicillin (100 units/mL), and streptomycin (100 μg/mL) in a humidified atmosphere of 5% CO_2/95% air at 37 °C. Cells were harvested and then centrifuged at 500*g*. The crude membranes were prepared after homogenization in 10 mM potassium phosphate, pH 7.4, and differential centrifugation at 48000*g* for 30 min at 4 °C. The pellets were washed twice in this manner before final resuspension in 10 mM potassium phosphate, pH 7.4, containing 100 mM potassium chloride.[57] [^{3}H]Flumazenil binding assays to transfected cells membranes were carried out as previously described.[57] In brief, the cell lines membranes were incubated in a volume of 500 μL, which contained [^{3}H]flumazenil at a concentration of 1−2 nM and the test compound in the range 10^{-9}−10^{-5} M. Nonspecific binding was defined by 10^{-5} M diazepam. Assays were incubated to equilibrium for 1 h at 4 °C.

Functional Efficacy Studies. $^{36}Cl^-$ uptake was measured in transfected HEK 293 cells stably expressing rat $GABA_A$ receptor subtypes ($\alpha_1\beta_2\gamma_2$, $\alpha_2\beta_2\gamma_2$), essentially as previously described.[29,35] In brief, coverlips were placed 8−10/cell culture plate (100 mm) and were incubated overnight under germicidal light in a solution containing 0.01 mg/mL polylysine in 0.1 M boric acid (pH 8.4). The following day, coverlips were washed twice with phosphate buffered saline and were placed into individual 6-well cell culture plates. DMEM/Nut Mix F-12 with Glut-I (GIBCO), supplemented with 10% fetal bovine serum, penicillin (100 units/mL), and streptomycin (100 μg/mL) were added to each well. Cells were then plated into each well at a density of 50×10^5 cells/well and were grown on the coverlips for 3 days at 37 °C with 5% CO_2. Cells were washed twice (10 s/wash) in wash buffer 136 mM NaCl, 5.4 mM KCl, 1.4 mM $MgCl_2$, 1.2 mM $CaCl_2$, 1 mM NaH_2PO_4, and 20 mM 4-(2-hydroxyethyl)-1-piperazin ethane sulfonic acid, adjusted to a pH of 7.4 with Tris base. All steps were conducted at room temperature. Cells were then dipped into 2 mL of a $^{36}Cl^-$ solution (2 μCi/mL) containing the drug to be studied, with or without GABA. Influx were terminated after 8 s by transfer coverlips to 500 mL ice-cold assay buffer (with 0.1 mM picrotoxin). Coverlips were drained rapidly and placed into 1.6 mL of 0.2 N NaOH in 20 mL scintillation vials and were left overnight. A 0.1 mL aliquot was removed and assayed for protein determination. The remaining 1.5 mL were neutralized with 0.3 mL of 1 N acetic acid and 20 mL of BioSafe II were added for counting by liquid scintillation spectrometry. Values for $^{36}Cl^-$ influx were expressed as nanomol/mg protein.

Pharmacology. Mouse Light/Dark Box Test. The experiments were carried out in accordance with the Animal Protection Law of the Republic of Italy, DL no. 116/1992, on the basis of the European Communities council Directive of 24 November 1986 (86/609/EEC). All efforts were made to minimize animal suffering and to reduce the number of animals involved ($n = 4$−6). Male CD-1 albino mice (35−40 g) (Harlan, Italy) were used. Ten mice were housed in cages under 12 h reversed lighting conditions (lights off at 2:00 and on at 14:00) in rooms held at constant temperature (22 ± 2 °C) and fed ad libitum on standard laboratory chow and tap water. After transfer from the breeding unit to the holding rooms, mice were allowed to acclimatize during 4 weeks to the reversed light cycle before the beginning of the experiments. Mice were only used once.

This test exploited the conflict between the animal's tendency to explore a new environment and its fear of bright light. Test for a change in anxiety were conducted essentially as described by Costall B. et al.[47] between 10.00−13.00 in a quiet darkened room illuminated by red light. The mice were taken from the dark holding rooms in a dark container to the experimental room. After 30 min, mice received ip either test compounds 20 mg/kg, or diazepam (Sigma) 1.25 mg/kg, or a vehicle (1% carboxymethyl cellulose). After a 1 h period of adaptation to the new environment, mice were placed into the test box. The open-topped test box (45cm × 27 cm × 27 cm high) had the floor area lined into 9 cm squares: two-fifths painted black illuminated under a red light (four red bulbs, each 15 W, 10 lx total) and the remainder of the box painted white and brightly illuminated with a 60 W (400 lx) light source. The compartments were separated by a divider and connected by an opening 7.5 cm × 7.5 cm located at the floor level in the center of the partition. Each mouse was tested by placing it in the center of the lit chamber, facing away from the dark one. The total duration of the test was 5 min. Each test was recorded on videotape, and the behavioral analysis was performed after recording. The time spent in the white compartment (TW) and the number of transfers from lit to dark areas and vice versa were measured. To obtain the total activity parameter, the number of exploratory rearings in the white section and the number of line crossings were measured.

Results are given as the mean ± SEM. Statistical analysis was performed using single-factor analysis of variance (ANOVA) and were appropriately followed by the procedure (Fisher's PLSD) for comparing the treatments to each other. Data were analyzed using the software StatView 5.0 Abacus Concept.

Computational Methods. Docking Simulations. The new version of the docking program AutoDock (version 4, AD4),[37] as implemented through the graphical user interface called AutoDockTools (ADT), was used to dock both **1c** and **2b** derivatives. This new release implements a new force field (FF) that, using an improved thermodynamic model of the binding process, allows inclusion of intramolecular terms in the estimated free energy. Moreover, the new FF includes a full desolvation model that contains terms for all atom types, including the favorable energetics of desolvating carbon atoms as well as the unfavorable energetics of desolvating polar and charged atoms. This FF also incorporates an improved model of directionality in hydrogen bonds, now predicting the proper alignment of groups with multiple hydrogen bonds. The structures of compounds **1c** and **2b** were built by using the Builder module in Insight2000.1 (Accelrys, San Diego, CA).[60] Atomic potentials and charges were assigned using the cvff force field.[61] Built conformations were geometrically optimized (Discover module, Insight2000.1) using a distance-dependent dielectric constant mimicking an aqueous environment ($\varepsilon = 80r$). Energy minimizations were performed using the conjugate gradient[62] as the minimization algorithm until the maximum rms derivative was less than 0.001 kcal mol−1 Å−1.

BzR structures that were kindly provided Cromer et al.[38] and by Ernst et al.[39] were energy minimized using Amber 9.0 software package.[40] Then the constructed compounds and BzR structure were converted to AD4 format files using ADT generating automatically all other atom values. The docking area was assigned visually around the ligands binding site. A grid of 60 Å × 60 Å × 60 Å with 0.375 Å spacing was calculated around the docking area for the ligand atom types using AutoGrid4. For each ligand, 100 separate docking calculations were performed. Each docking calculation consisted of 10 million energy evaluations using the Lamarckian genetic algorithm local search (GALS) method. The GALS method evaluates a population of possible docking solutions and propagates the most successful individuals from each generation into the subsequent generation of possible solutions. A low-frequency local search according to the method of Solis and Wets is applied to docking trials to ensure that the final solution represents a local minimum. All dockings described in this paper were performed with a population size of 250, and 300 rounds of Solis and Wets local search were applied with a probability of 0.06. A mutation rate of 0.02 and a crossover rate of 0.8 were used to generate new docking trials for subsequent generations, and the best individual from each generation was propagated over the next generation. The docking results from each of the 100 calculations were clustered on the basis of root-mean-square deviation (rmsd) (solutions differing by less than 2.0 Å) between the Cartesian coordinates of the atoms and were ranked on the basis of free energy of binding (ΔG_{AD4}). The top-ranked compounds were visually inspected for good chemical geometry.

Molecular Dynamics and Energy Minimization Simulations. The binary complexes between BzR and **2b** and**1c** in both binding mode A and B were investigated by means of MD

simulations carried out with the AMBER 9.0 package software.[40] Ligand force-field parameters were derived using the Antechamber program,[63] and partial charges for the substrates were derived using the AM1-BCC procedure in Antechamber. Eleven ns MD simulations on the aforementioned four complexes were carried out in explicit solvent and periodic boundary conditions. One Cl^- counterion was added to the solvent bulk of the protein−water complexes to maintain neutrality in the systems. First, water shells and counterion were minimized using steepest descent and conjugate gradient algorithms. Then a minimization of the entire ensemble was performed setting a convergence criterion on the gradient of 0.001 kcal mol^{-1} $Å^{-1}$. Equilibration runs were carried out by heating the system to 300 K in 1 ns. This was followed by 10 ns MD simulations in the NPT ensemble (constant temperature and pressure). The parm99 version[64] of the all-atom Amber force field[65] was used for the protein and the counterion, whereas the TIP3P model[66] was employed to explicitly represent water molecules. van der Waals and short-range electrostatic interactions were estimated within a 10 Å cutoff, whereas the long-range electrostatic interactions were assessed by using the particle mesh Ewald (PME) method,[67] with a 1 Å charge grid spacing interpolated by a fourth-order B-spline, and by setting the direct sum tolerance to 10^{-5}. Bonds involving hydrogen atoms were constrained by using the SHAKE algorithm[68] with a relative geometric tolerance for coordinate resetting of 0.00001 Å. Berendsen's coupling algorithms[69] were employed to maintain constant temperature and pressure with the same scaling factor for both solvent and solutes and with the time constant for heat bath coupling maintained at 1.5 ps. The pressure for the isothermal−isobaric ensemble was regulated by using a pressure relaxation time of 1 ps in Berendsen's algorithm. The simulations of the solvated protein models were performed using a constant pressure of 1 atm and a constant temperature of 300 K. Analysis of MD trajectories was attained using the ptraj software.[70] This software was also used to calculate the average structures of the four complexes that were energy minimized by employing the same geometrical optimization protocol mentioned above. All calculations were performed on a Linux machine employing a Fedora Core 7 architecture.

Acknowledgment. We are grateful to Prof. Cromer and Prof. Ernst for kindly providing the homology models of the $\alpha_1\beta_2\gamma_2$ $GABA_A$ receptor. Furthermore, we thank Dr. François Besnard for his generous gift of HEK293 cells stably expressing rat $GABA_A$ receptor subtypes ($\alpha_1\beta_2\gamma_2$, $\alpha_2\beta_2\gamma_2$, $\alpha_5\beta_3\gamma_2$).

Supporting Information Available: Tables including physical properties, spectral and analytical data of compounds **3c**−**j**,Tables reporting the ΔG_{AD4} calculated for the ligand/BzR complexes, together with additional molecular modeling pictures. This material is available free of charge via the Internet at http://pubs.acs.org.

References

(1) Sigel, E. Mapping of the Benzodiazepine Recognition Site on $GABA_A$ Receptors. *Curr. Top. Med. Chem.* **2002**, *2*, 833–839.
(2) Teuber, L.; Watjens, F.; Jensen, L. H. Ligands for the Benzodiazepine Binding Site-A Survey. *Curr. Pharm. Des.* **1999**, *5*, 317–343.
(3) Gardner, C. R. Interpretation of the Behavioral Effects of Benzodiazepine Receptor Ligands. *Drugs Future* **1989**, *14*, 51–67.
(4) Sieghart, W. Structure and Pharmacology of γ-Aminobutyric $Acid_A$ Receptor Subtypes. *Pharmacol. Rev.* **1995**, *47*, 181–234.
(5) Chebib, M.; Johnston, G. A. R. GABA-Activated Ligand Gated Ion Channels: Medicinal Chemistry and Molecular Biology. *J. Med. Chem.* **2000**, *43*, 1427–1447.
(6) Mehta, A. K.; Ticku, M. K. An Update on GABA-A Receptors. *Brain Res. Rev.* **1999**, *29*, 196–217.
(7) Sieghart, W.; Sperk, G. Subunit Composition, Distribution and Function of GABA(A) Receptor Subtypes. *Curr. Top. Med. Chem.* **2002**, *2*, 795–816.
(8) Mohler, H.; Fritschy, J. M.; Rudolph, U. A New Benzodiazepine Pharmacology. *J. Pharmacol. Exp. Ther.* **2002**, *300*, 2–8.
(9) Whiting, P. J. GABA-A Receptor Subtypes in the Brain: A Paradigm for CNS Drug Discovery. *Drug Discovery Today* **2003**, *8*, 445–450.
(10) Da Settimo, F.; Taliani, S.; Trincavelli, M. L.; Montali, M.; Martini, C. $GABA_A$/Bz Receptor Subtypes as Targets for Selective Drugs. *Curr. Med. Chem.* **2007**, *14*, 2680–2701.
(11) Atack, J. R. The Benzodiazepine Binding Site of $GABA_A$ Receptors as a Target for the Development of Novel Anxiolytics. *Expert. Opin. Invest. Drugs* **2005**, *14*, 601–618.
(12) Zhang, W.; Koehler, K. F.; Zhang, P.; Cook, J. M. Development of a Comprehensive Pharmacophore Model for the Benzodiazepine Receptor. *Drug Des. Discovery* **1995**, *12*, 193–248.
(13) Huang, Q.; He, X.; Ma, C.; Liu, R.; Yu, S.; Dayer, C. A.; Wenger, G. R.; McKernan, R.; Cook, J. M. Pharmacophore/Receptor Models for $GABA_A$/BzR Subtypes ($\alpha_1\beta_3\gamma_2$, $\alpha_5\beta_3\gamma_2$, and $\alpha_6\beta_3\gamma_2$) via a Comprehensive Ligand-Mapping Approach. *J. Med. Chem.* **2000**, *43*, 71–95.
(14) He, X.; Huang, Q.; Ma, C.; Yu, S.; McKernan, R.; Cook, J. M. Pharmacophore/Receptor Models for $GABA_A$/BzR $\alpha_2\beta_3\gamma_2$, $\alpha_3\beta_3\gamma_2$, and $\alpha_4\beta_3\gamma_2$ Recombinant Subtypes. Included Volume Analysis and Comparison to $\alpha_1\beta_3\gamma_2$, $\alpha_5\beta_3\gamma_2$, and $\alpha_6\beta_3\gamma_2$. *Drug Des. Discovery* **2000**, *17*, 131–171.
(15) Yu, S.; He, X.; Ma, C.; McKernan, R.; Cook, J. M. Studies in Search of α2 Selective Ligands for $GABA_A$/BzR Receptor Subtypes. Part I. Evidence for the Conservation of Pharmacophoric Descriptors for DS Subtypes. *Med. Chem. Res* **1999**, *9*, 186–202.
(16) Collins, I.; Moyes, C.; Davey, W. B.; Rowley, M.; Bromidge, F. A.; Quirk, K.; Atack, J. R.; McKernan, R. M.; Thompson, S. A.; Wafford, K.; Dawson, G. R.; Pike, A.; Sohal, B.; Tsou, N. N.; Ball, R. G.; Castro, J. L. 3-Heteroaryl-2-pyridones: Benzodiazepine Site Ligands with Functional Selectivity for α2/α3-Subtypes of Human $GABA_A$ Receptor-Ion Channels. *J. Med. Chem.* **2002**, *45*, 1887–1900.
(17) Loughhead, D. G.; Novakovic, S.; O'Yang, C.; Putman, D. G.; Soth, M. Preparation of Pyrazolopyridines and Other Heterocycle-fused Pyrazoles as $GABA_A$ α2 Subtype Selective Receptor Modulators. PCT Int. Appl. WO 2005077363 A1, 2005.
(18) Atack, J. R.; Wafford, K. A.; Tye, S. J.; Cook, S. M.; Sohal, B.; Pike, A.; Sur, C.; Melillo, D.; Bristow, L.; Bromidge, F.; Ragan, I.; Kerby, J.; Street, L.; Carling, R.; Castro, J. L.; Whiting, P.; Dawson, G. R.; McKernan, R. M. TPA023 [7-(1,1-Dimethylethyl)-6-(2-ethyl-2*H*-1,2,4-triazol-3-ylmethoxy)-3-(2-fluorophenyl)-1,2,4-triazolo[4,3-*b*]pyridazine], an Agonist Selective for α2- and α3-containing $GABA_A$ Receptors, Is a Nonsedating Anxiolytic in Rodents and Primates. *J. Pharmacol. Exp. Ther.* **2006**, *316*, 410–422.
(19) Griebel, G.; Perrault, G.; Simiand, J.; Cohen, C.; Granger, P.; Decobert, M.; Françon, D.; Avenet, P.; Depoortere, H.; Tan, S.; Oblin, A.; Schoemaker, H.; Evanno, Y.; Sevrin, M.; George, P.; Scatton, B. SL651498: An Anxioselective Compound with Functional Selectivity for α2- and α3-containing γ-aminobutyric $acid_A$ ($GABA_A$) Receptors. *J. Pharmacol. Exp. Ther.* **2001**, *298*, 753–768.
(20) Licata, S. C.; Platt, D. M.; Cook, J. M.; Sarma, P. V.; Griebel, G.; Rowlett, J. K. Contribution of $GABA_A$ Receptor Subtypes to the Anxiolytic-Like, Motor, and Discriminative Stimulus Effects of Benzodiazepines: Studies with the Functionally Selective Ligand SL651498 [6-Fluoro-9-methyl-2-phenyl-4-(pyrrolidin-1-yl-carbonyl)-2,9-dihydro-1*H*-pyridol[3,4-*b*]indol-1-one]. *J. Pharmacol. Exp. Ther.* **2005**, *313*, 1118–1125.
(21) Crawforth, J.; Atack, J. R.; Cook, S. M.; Gibson, K. R.; Nadin, A.; Owens, A. P.; Pike, A.; Rowley, M.; Smith, A. J.; Sohal, B.; Sternfeld, F.; Wafford, K.; Street, L. J. Tricyclic Pyridones as Functionally Selective Human $GABA_A\alpha_{2/3}$ Receptor−Ion Channel Ligands. *Bioorg. Med. Chem. Lett.* **2004**, *14*, 1679–1682.
(22) Albaugh, P. A.; Marshall, L.; Gregory, J.; White, G.; Hutchinson, A.; Ross, P. C.; Gallagher, D. W.; Tallman, J. F.; Crago, M.; Cassella, J. V. Synthesis and Biological Evaluation of 7,8,9,10-Tetrahydroimidazo[1,2-*c*]pyrido[3,4-*e*]pyrimidin-5(6*H*)-ones as Functionally Selective Ligands of the Benzodiazepine Receptor Site on the $GABA_A$ Receptor. *J. Med. Chem.* **2002**, *45*, 5043–5051.
(23) Russell, M. G. N.; Carling, R. W.; Atack, J. R.; Bromidge, F. A.; Cook, S. M.; Hunt, P.; Isted, C.; Lucas, M.; McKernan, R. M.; Mitchinson, A.; Moore, K. W.; Narquizian, R.; Macaulay, A. J.; Thomas, D.; Thompson, S. A.; Wafford, K. A.; Castro, J. L. Discovery of Functionally Selective 7,8,9,10-Tetrahydro-7,10-ethano-1,2,4-triazolo[3,4-*a*]phthalazines as $GABA_A$ Receptor Agonists at the α_3 Subunit. *J. Med. Chem.* **2005**, *48*, 1367–1383.
(24) Blackaby, W. P.; Atack, J. R.; Bromidge, F.; Lewis, R.; Russel, M. G. N.; Smith, A.; Wafford, K.; McKernan, R. M.; Street, L. J.; Castro, J. L. Pyrazolopyridinones as Functionally Selective $GABA_A$ Ligands. *Bioorg. Med. Chem. Lett.* **2005**, *15*, 4998–5002.
(25) Goodacre, S. C.; Street, L. J.; Hallett, D. J.; Crawforth, J. M.; Kelly, S.; Owens, A. P.; Blackaby, W. P.; Lewis, R. T.; Stanley, J.; Smith, A. J.; Ferris, P.; Sohal, B.; Cook, S. M.; Pike, A.; Brown, N.; Wafford, K. A.; Marshall, G.; Castro, J. L.; Atack, J. R. Imidazo[1,2-*a*]-

pyrimidines as Functionally Selective and Orally Bioavailable $GABA_A$ α_2/α_3 Binding Site Agonists for the Treatment of Anxiety Disorders. *J. Med. Chem.* **2006**, *49*, 35–38.

(26) Da Settimo, A.; Primofiore, G.; Da Settimo, F.; Marini, A. M.; Novellino, E.; Greco, G.; Martini, C.; Giannaccini, G.; Lucacchini, A. Synthesis, Structure−Activity Relationships, and Molecular Modeling Studies of *N*-(Indol-3-ylglyoxylyl)benzylamine Derivatives Acting at the Benzodiazepine Receptor. *J. Med. Chem.* **1996**, *39*, 5083–5091.

(27) Primofiore, G.; Da Settimo, F.; Taliani, S.; Marini, A. M.; Novellino, E.; Greco, G.; Lavecchia, A.; Besnard, F.; Trincavelli, L.; Costa, B.; Martini, C. Novel *N*-(Arylalkyl)indol-3-ylglyoxylylamides Targeted as Ligands of the Benzodiazepine Receptor: Synthesis, Biological Evaluation, and Molecular Modeling Analysis of the Structure−Activity Relationships. *J. Med. Chem.* **2001**, *44*, 2286–2297.

(28) Da Settimo, A.; Primofiore, G.; Da Settimo, F.; Marini, A. M.; Novellino, E.; Greco, G.; Gesi, M.; Martini, C.; Giannaccini, G.; Lucacchini, A. *N*′-Phenylindol-3-ylglyoxylohydrazide Derivatives: Synthesis, Structure−Activity Relationships, Molecular Modeling Studies, and Pharmacological Action on Brain Benzodiazepine Receptors. *J. Med. Chem.* **1998**, *41*, 3821–3830.

(29) Primofiore, G.; Taliani, S.; Da Settimo, F.; Marini, A. M.; La Motta, C.; Simorini, F.; Patrizi, M. P.; Sergianni, V.; Novellino, E.; Greco, G.; Cosimelli, B.; Calderone, V.; Montali, M.; Besnard, F.; Martini, C. Novel *N*-Substituted Indol-3-ylglyoxylamides Probing the L_{Di} and L_1/L_2 Lipophilic Regions of the Benzodiazepine Receptor Site in Search for Subtype-Selective Ligands. *J. Med. Chem.* **2007**, *50*, 1627–1634.

(30) Da Settimo, A.; Primofiore, G.; Marini, A. M.; Ferrarini, P. L.; Franzone, J. S.; Cirillo, L.; Reboani, M. C. *N*-(Indol-3ylglyoxylyl) -methionine Derivatives: Preparation and Gastric Antisecretory Activity. *Eur. J. Med. Chem.* **1988**, *23*, 21–24.

(31) Soerensen, U. S.; Teuber, L.; Peters, D.; Stroebaek, D.; Johansen, T. H.; Nielsen, K. S.; Christophersen, P. Preparation of Novel 2-Aminobenzimidazole Derivatives as Modulators of Small-Conductance Calcium-Activated Potassium Channels. PCT Int. Appl. WO 2006013210 A2, 2006.

(32) Borne, R. F.; Forrester, M. L.; Waters, I. W. Conformational Analogues of Antihypertensive Agents Related to Guanethidine. *J. Med. Chem.* **1977**, *20*, 771–776.

(33) Gomtsyan, A.; Bayburt, E. K.; Lee, C.-H.; Koenig, J. R.; Schmidt, R.; Lukin, K.; Chambournier, G.; Hsu, M.; Leanna, M. R.; Cink, R. D. Preparation of Fused Heterocyclic Compounds as Vanilloid Receptor Subtype 1 (VR1) Inhibitors. PCT Int. Appl. WO 2004111009 A1, 2004.

(34) Giannaccini, G.; Giacomelli, M.; Martini, C.; Lucacchini, A.; Piccolino, M. Binding of the Benzodiazepine Ligand [^{3}H]Ro 15-1788 to Membrane Preparations of the Rabbit and Turtle Retina. *Comp. Biochem. Physiol., Part C: Toxicol. Pharmacol.* **1992**, *101*, 337–342.

(35) Harris, R. A.; Proctor, W. R.; McQuilkin, S. J.; Klein, R. L.; Mascia, M. P.; Whatley, V.; Whiting, P. J.; Dunwiddie, T. V. Ethanol Increases $GABA_A$ Responses in Cells Stably Transfected with Receptor Subunits. *Alcohol.: Clin. Exp. Res.* **1995**, *19*, 226–232.

(36) Street, L. J.; Sternfeld, F.; Jelley, R. A.; Reeve, A. J.; Carling, R. W.; Moore, K. W.; McKernan, R. M.; Sohal, B.; Cook, S.; Pike, A.; Dawson, G. R.; Bromidge, F. A.; Wafford, K. A.; Seabrook, G. R.; Thompson, S. A.; Marshall, G.; Pillai, G. V.; Castro, J. L.; Atack, J. R.; MacLeod, A. M. Synthesis and Biological Evaluation of 3-Heterocyclyl-7,8,9,10-tetrahydro-(7,10-ethano)-1,2,4-triazolo[3,4-*a*]phthalazines and Analogues as Subtype-Selective Inverse Agonists for the $GABA_A\alpha_5$ Benzodiazepine Binding Site. *J. Med. Chem.* **2004**, *47*, 3642–3657.

(37) Huey, R.; Morris, G. M.; Olson, A. J.; Goodsell, D. S. A Semiempirical Free Energy Force Field with Charge-Based Desolvation. *J. Comput. Chem.* **2007**, *28*, 1145–1152.

(38) Cromer, B. A.; Morton, C. J.; Parker, M. W. Anxiety over GABA(A) Receptor Structure Relieved by AChBP. *Trends Biochem. Sci.* **2002**, *27*, 280–287.

(39) Ernst, M.; Bruckner, S.; Boresch, S.; Sieghart, W. Comparative models of $GABA_A$ Receptor Extracellular and Transmembrane Domains: Important Insights in Pharmacology and Function. *Mol. Pharmacol.* **2005**, *68*, 1291–1300.

(40) Case, D. A.; Darden, T. E.; Cheatham, T. E. I.; Simmerling, C. L.; Wang, J.; Duke, R. E.; Luo, R.; Merz, K. M., Wang, B.; Pearlman, D. A.; Crowley, M.; Brozell, S.; Tsui, V.; Gohlke, H.; Mongan, J.; Hornak, V.; Cui, G.; Beroza, P.; Schafmeister, C.; Caldwell, J. W.; Ross, W. S.; Kollman, P. A. , *AMBER 9*; University of California: San Francisco.

(41) Sanner, M. F.; Python, A. Programming Language for Software Integration and Development. *J. Mol. Graphics Modell.* **1999**, *17*, 57–61.

(42) Pettersen, E. F.; Goddard, T. D.; Huang, C. C.; Couch, G. S.; Greenblatt, D. M.; Meng, E. C.; Ferrin, T. E. UCSF Chimera−A Visualization System for Exploratory Research and Analysis. *J. Comput. Chem.* **2004**, *25*, 1605–1612.

(43) Primofiore, G.; Da Settimo, F.; Marini, A. M.; Taliani, S.; La Motta, C.; Simorini, F.; Novellino, E.; Greco, G.; Cosimelli, B.; Ehlardo, M.; Sala, A.; Besnard, F.; Montali, M.; Martini, C. Refinement of the Benzodiazepine Receptor Site Topology by Structure−Activity Relationships of New *N*-(Heteroarylmethyl)indol-3-ylglyoxylamides. *J. Med. Chem.* **2006**, *49*, 2489–2495.

(44) McKernan, R. M.; Rosahl, T. W.; Reynolds, D. S.; Sur, C.; Wafford, K. A.; Atack, J. R.; Farrar, S.; Myers, J.; Cook, G.; Ferris, P.; Garrett, L.; Bristow, L.; Marshall, G.; Macaulay, A.; Brown, N.; Howell, O.; Moore, K. W.; Carling, R. W.; Street, L. J.; Castro, J. L.; Ragan, C. I.; Dawson, G. R.; Whi, P. J. Sedative but not Anxiolytic Properties of Benzodiazepines are Mediated by the $GABA_A$ Receptor α_1 Subtype. *Nat. Neurosci.* **2000**, *3*, 587–592.

(45) Bourin, M.; Hascoët, M. The Mouse Light/Dark Box Test. *Eur. J. Pharmacol.* **2003**, *463*, 55–65.

(46) Hascoët, M.; Bourin, M. A New Approach to the Light/Dark Test Procedure in Mice. *Pharmacol., Biochem. Behav.* **1998**, *60*, 645–653.

(47) Costall, B.; Jones, B. J.; Kelly, M. E.; Naylor, R. J.; Tomlins, D. M. Exploration of Mice in a Black and White Test Box: Validation as a Model of Anxiety. *Pharmacol., Biochem. Behav.* **1989**, *32*, 777–785.

(48) Kilfoil, T.; Michel, A.; Montgomery, D.; Whiting, R. L. Effects of Anxiolytic and Anxiogenic Drugs on Exploratory Activity in a Simple Model of Anxiety in Mice. *Neuropharmacology* **1989**, *28*, 901–905.

(49) Young, R.; Johnson, D. N. A Fully Automated Light/Dark Apparatus Useful for Comparing Anxiolytic Agents. *Pharmacol., Biochem. Behav.* **1991**, *40*, 739–743.

(50) Clayton, T.; Chen, J. L.; Ernst, M.; Richter, L.; Cromer, B. A.; Morton, C. J.; Ng, H.; Kaczorowski, C. C.; Helmstetter, F. J.; Furtmüller, R.; Ecker, G.; Parker, M. W.; Sieghart, W.; Cook, J. M. An Updated Unified Pharmacophore Model of the Benzodiazepine Binding Site on γ-Aminobutyric $Acid_a$ Receptors: Correlation with Comparative Models. *Curr. Med. Chem.* **2007**, *14*, 2755–2775.

(51) Zhang, W.; Diaz-Arauzo, H.; Allen, M. S.; Koehler, K. F.; Cook, J. M. Chemical and Computer Assisted Development of the Inclusive Pharmacophore of Benzodiazepine Receptors. In *Studies in Medicinal Chemistry*; ChoudharyM. I., Ed.; Harwood Academic Publishers: Chichester, U.K., 1996; pp 303.

(52) Buhr, A.; Baur, R.; Malherbe, P.; Sigel, E. Point Mutations of the $\alpha 1\beta 2\gamma 2$ γ-aminobutyric $acid_A$ Receptor Affecting Modulation of the Channel by Ligands of the Benzodiazepine Binding Site. *Mol. Pharmacol.* **1996**, *49*, 1080–1084.

(53) Sigel, E.; Baur, R.; Trube, G.; Möhler, H.; Malherbe, P. The Effect of Subunit Composition of Rat Brain $GABA_A$ Receptors on Channel Function. *Neuron* **1990**, *5*, 703–711.

(54) Sawyer, G. W.; Chiara, D. C.; Olsen, R. W.; Cohen, J. B. Identification of the Bovine γ-Aminobutyric Acid Type A Receptor α Subunit Residues Photolabeled by the Imidazobenzodiazepine [^{3}H]Ro15-4513. *J. Biol. Chem.* **2002**, *277*, 50036–50045.

(55) Da Settimo, A.; Primofiore, G.; Da Settimo, F.; Marini, A. M.; Novellino, E.; Greco, G.; Martini, C.; Senatore, G.; Lucacchini, A. Synthesis of 3-(2′-Furoyl)indole Derivatives as Potential New Ligands at the Benzodiazepine Receptor, Structurally More Restrained Analogues of Indoleglyoxylylamides. *Farmaco* **1995**, *50*, 311–320.

(56) Miller, R. B.; Frincke, J. M. Synthesis of Isoquinolines from Indenes. *J. Org. Chem.* **1980**, *45*, 5312–5315.

(57) Besnard, F.; Even, Y.; Itier, V.; Granger, P.; Partiseti, M.; Avenet, P.; Depoortere, H.; Graham, D. Development of Stable Cell Lines Expressing Different Subtypes of $GABA_A$ Receptors. *J. Recept. Signal Transduction Res.* **1997**, *17*, 99–113.

(58) Martini, C.; Lucacchini, A.; Ronca, G.; Hrelia, S.; Rossi, C. A. Isolation of Putative Benzodiazepine Receptors From Rat Brain Membranes by Affinity Chromatography. *J. Neurochem.* **1982**, *38*, 15–19.

(59) Lowry, O. H.; Rosebrough, N. J.; Farr, A. L.; Randall, R. J. Protein Measurement With the Folin Phenol Reagent. *J. Biol. Chem.* **1951**, *193*, 265–275.

(60) Accelrys, Inc., San Diego, CA.

(61) Dauber-Osguthorpe, P.; Roberts, V. A.; Osguthorpe, D. J.; Wolff, J.; Genest, M.; Hagler, A. T. Structure and energetics of ligand binding to proteins. *Proteins: Struct., Funct., Genet.* **1988**, *4*, 31−47.

(62) Fletcher, R. Unconstrained Optimization. In *Practical Methods of Optimization*; John Wiley & Sons: New York, 1980; Vol. 1.

(63) Wang, J.; Wolf, R. M.; Caldwell, J. W.; Kollman, P. A.; Case, D. A. Development and Testing of a General Amber Force Field. *J. Comput. Chem.* **2004**, *25*, 1157–1174.

(64) Wang, J.; Cieplak, P.; Kollman, P. A. How Well Does a Restrained Electrostatic Potential (RESP) Model Perform in Calculating Conformational Energies of Organic and Biological Molecules? *J. Comput. Chem.* **2000**, *21*, 1049–1074.
(65) Cornell, W. D.; Cieplak, P.; Bayly, C. I.; Gould, I. R.; Merz, K. M.; Ferguson, D. M.; Spellmeyer, D. C.; Fox, T.; Caldwell, J. W.; Kollman, P. A. A Second Generation Force Field for the Simulation of Proteins, Nucleic Acids, and Organic Molecules. *J. Am. Chem. Soc.* **1995**, *117*, 5179–5197.
(66) Jorgensen, W. L.; Chandrasekhar, J.; Madura, J. D.; Impey, R. W.; Klein, L. M. Comparison of Simple Potential Functions for Simulating Liquid Water. *J. Chem. Phys.* **1983**, *79*, 926–935.
(67) Essmann, U.; Perera, L.; Berkowitz, M. L.; Darden, T.; Lee, H.; Pedersen, L. G. A Smooth Particle Mesh Ewald Method. *J. Chem. Phys.* **1995**, *103*, 8577–8593.
(68) Ryckaert, J. P.; Ciccotti, G.; Berendsen, H. J. C. Numerical Integration of the Cartesian Equations of Motion of a System with Constraints: Molecular Dynamics of *n*-Alkanes. *J. Comput. Phys.* **1977**, *23*, 327–341.
(69) Berendsen, H. J. C.; Postma, J. P. M.; Van Gunsteren, W. F.; Di Nola, A.; Haak, J. R. Molecular Dynamics with Coupling to an External Bath. *J. Chem. Phys.* **1984**, *81*, 3684–3690.
(70) Shao, J.; Tanner, S. W.; Thompson, N.; Cheatham, T. E. I. Clustering Molecular Dynamics Trajectories: I. Characterizing the Performance of Different Clustering Algorithms. *J. Chem. Theory Comput.* **2007**, *3*, 2312–2334.

JM9001154